Core Edge Inset Radius Variation Technique To Reduce Cogging Torque Of Interior Permanent Magnet Synchronous Motors

Tanuj Jhankal, Amit N. Patel

Abstract: In spite of various advantages, permanent magnet synchronous motors have a major disadvantage of high cogging torque. It is very necessary to bring down this high cogging torque to enhance overall performance of the interior permanent magnet synchronous motor (IPMSM). This paper presents core edge inset radius variation technique for the reduction of cogging torque in IPMSMs. The effect of changing core-edge inset radius (CEIR) on the cogging torque of IPMSMs has been analyzed in three different three-phase, 4-pole/12-slot IPMSM configurations having the different envelope dimensions for high-speed applications. To check the effectiveness of proposed technique for wide range of applications three different standard rating IPMSMs are considered for analysis. Finite element analysis is used for motor characteristics reckoning. Effective reduction is observed in cogging torque by using core edge inset radius variation technique in three standard rating IPMSMs. It is indispensable to choose the proper value of the core edge inset radius of IPMSMs during design stage for reduced cogging torque.

Index Terms: Cogging Torque, Computer Aided Design, Core Edge Inset Radius, Finite Element Analysis, Interior Permanent Magnet Synchronous Motor, spoke-type PM.

1. INTRODUCTION

PERMANENT magnet (PM) motors are in very much use in various applications due to high efficiency, compact size and fast dynamic response. As new researches are carried out in designing and development of PM motors, this has made more utilization of PM motors in aerospace, electrical vehicles, domestic and industrial applications [1], [2], [3]. A permanent magnet motor includes a stator having core and teeth with the coil wound on it; a rotor is provided concentrically inside the stator. Instead of electromagnetic excitation application of permanent magnets in the motor have many advantages so the rotor is provided with permanent magnet poles. The popularity of PM motor design is expanding continuously and become a point of interest for the designers due to the accessibility of rare earth permanent magnets with high energy density, easily magnetized rectangular shaped magnets and developments in semiconductor devices [4]. There are two types of permanent magnet motors based on the placement of magnet on rotor core: surface permanent magnet (SPM) type motor and interior permanent magnet (IPM) type motor. Fig. 1 illustrates basic rotor configurations i.e. IPM and SPM. Compared with surface permanent magnet type motor, interior permanent magnet motors have clear advantages in many ways. First, the manufacturing process is not complex and has high reliability because magnets can be directly embedded in the rotor without binding material needed. Second, in IPM motors significant reluctance torque can be obtained.

- *Tanuj Jhankal Assistant Professor, Department of Electrical Engineering, Jaipur Engineering College, Jaipur, India. E-mail: tanuj.jhankaljec@gmail.com*
- *Amit N. Patel Assistant Professor, Department of Electrical Engineering, Institute of Technology, Nirma University, Ahmedabad, India E-mail: amit.patel@nirmauni.ac.in (corresponding author)*

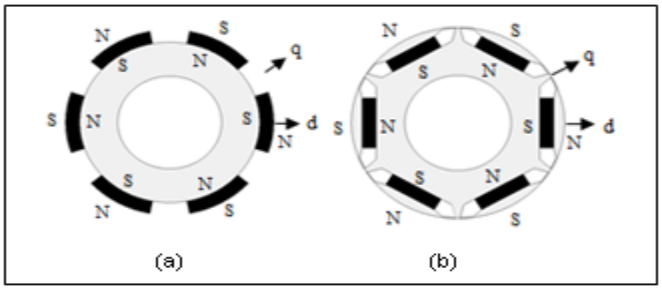

***Fig. 1**. Shows basic rotor configuration of (a) SPM and (b) IPM.*

Third, as the magnets are not exposed to the air gap directly the demagnetization risk is low. Fourth, permanent magnet materials are more efficiently used. Since the rectangular shape of magnets is used. This cause an increase in the rate of acceptance of IPM motors for industrial applications. Interior permanent magnet synchronous motors are progressively becoming popular nowadays in different torque quality sensitive applications like electric vehicle, elevators and servo drives. One of the biggest problems of IPMSM cogging torque as it deteriorates the quality of torque and also introduces vibration in motor. Due to presence of slotted stator and permanent magnets cogging torque is inherent in PMSM. Cogging torque is regarded as interaction between rotor mmf and air-gap permeance variation. There have been several techniques and effective approaches which are proposed for the reduction of cogging torque in the past few decades. A large variety of approaches or techniques can be used in design optimization of both rotor and stator. For stator part, optimization can be done on tooth width variation [5], width of slot opening [6], tooth shifting [7], stator dummy slot addition [8] and skewing [9], [10], [11], [12]. Similarly, cogging torque can also be reduced by optimization of the rotor side. Many techniques are employed for optimization using rotor parameters, e.g. magnet sizing, shifting of magnets [13], pole arc width variation [8], [14], [15], pole shaping and shifting [9], [16] and rotor skewing [9], [10], [14], etc. are some of the techniques which are extensively in use to solve cogging torque problem. The most common techniques used are stator skewing and step skewing of the rotor. Skewing can reduce cogging torque dramatically, but also

produce an unwanted and unexpected axial force [17]. Lower value of cogging torque is provided by step-skewed rotor technique Inherently but it still have some issues like axial interaction between rotor steps, end leakage flux and manufacturing tolerances influence arising due to skewed rotor side [18]. And another problem is regarding construction because it is complicated to fabricate a stator with skewed stator teeth and similar for the rotor side it is difficult to produce and magnetize a skewed magnet [18]. This paper proposes the core-edge inset radius (CEIR) variation technique for IPMSM to reduce the cogging torque. The partly round core edge, made by modifying the rotor's core structure is introduced. This technique does not require any kind of modification in magnet and/or construction of dummy slots, which makes the rotor construction quiet easier then rotors for different techniques like step-skewed, pole shifting, etc. Section II provides the information about the initial design of IPMSMs which includes the rating, type of motor, type of magnet used and other design parameters for three different rating motors. Section III discusses cogging torque and provides basic information regarding the cause of the generation of cogging torque. Effect of CEIR variation on the performance of three different ratings IPMSMs is discussed in section IV. While section V concludes the work done in this paper.

2. INITIAL DESIGN OF IPMSM

Three standard rating IPMSMs of (i) 2 kW, (ii) 5 kW and (iii) 120 kW are designed initially. Finite element (FE) models of these motors have been created based on design details are illustrated in Fig. 1.

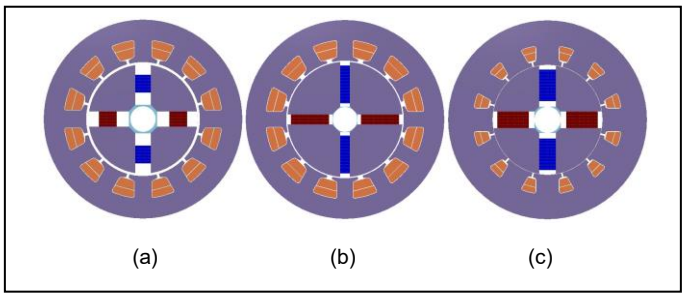

***Fig. 2**. Showing cross-sectional view of initial IPMSM models (a) 2 kW model, (b) 5 kW model and (c) 120 kW model.*

Design details of three initially designed motors are shown in Table. 1. All three interior PMSMs consist same number of stator slots and rotor pole of interior permanent magnet rotor pole structure and three phase winding on the stator side. With the magnetization in alternately reversing polarity NdFeB (Neo-dymium Iron Boron) grade 35 permanent magnets are utilized and arranged in a spoke-type array like structure to form rotor poles. Salient properties of 35 grade NdFeB are as under:

1. Flux (residual) density: 1.23 T
2. Maximum value of energy product: 35 MGOe
3. Coercive force: 890 KA/m
4. Relative permeability:1.0

TABLE 1

INITIAL DESIGN DETAILS

Item	Unit	Motor 1	Motor 2	Motor 3
Stator outer diameter	mm	40.5	88.1	364
Stator inner diameter	mm	23.2	52.1	201
Stator back iron depth	mm	4.06	8.77	45
Stator tooth width	mm	3.5	6.82	42
Slots/Pole/Phase	-	1	1	1
No. of phases	-	3	3	3
No. of poles	-	4	4	4
No. of stator slots	-	12	12	12
Axial length	mm	24.3	51.08	200
Air-gap length	mm	0.5	0.5	0.5
Rotor outer diameter	mm	22.2	51.08	200
Core material	-	M19	M19	M19
Type of PM	-	N35	N35	N35

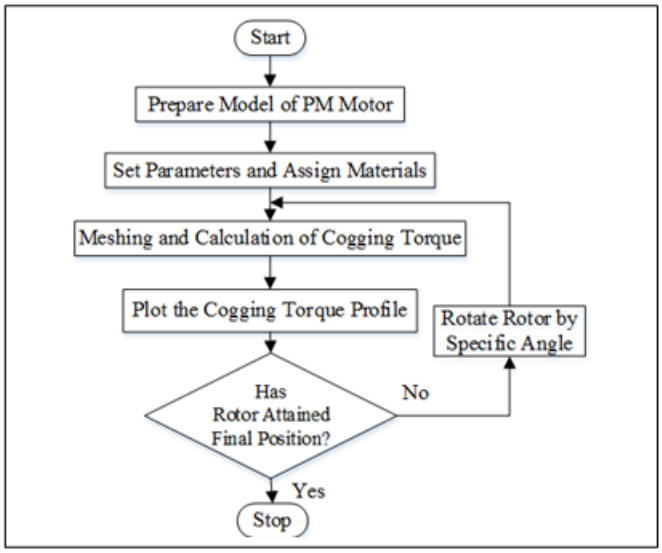

***Fig. 3**. Flow chart to determine cogging torque profile.*

And non-oriented silicon steel M19 is used as material for stator core, teeth and rotor core design. The space factor is kept the same 0.4 in all the initial models. Initial designs are considered as reference designs for performance comparison and analysis. The improved models have similar air-gap length and rotor outer diameter. Finite element models are created based on design information and proper materials are assigned. Meshing is done with triangular elements and boundary conditions are assigned. At particular rotor position cogging torque is obtained with FEA. This process is continued till final position for each incremental rotor position. Flow chart for this series of simulation exercise is shown in Fig. 3.

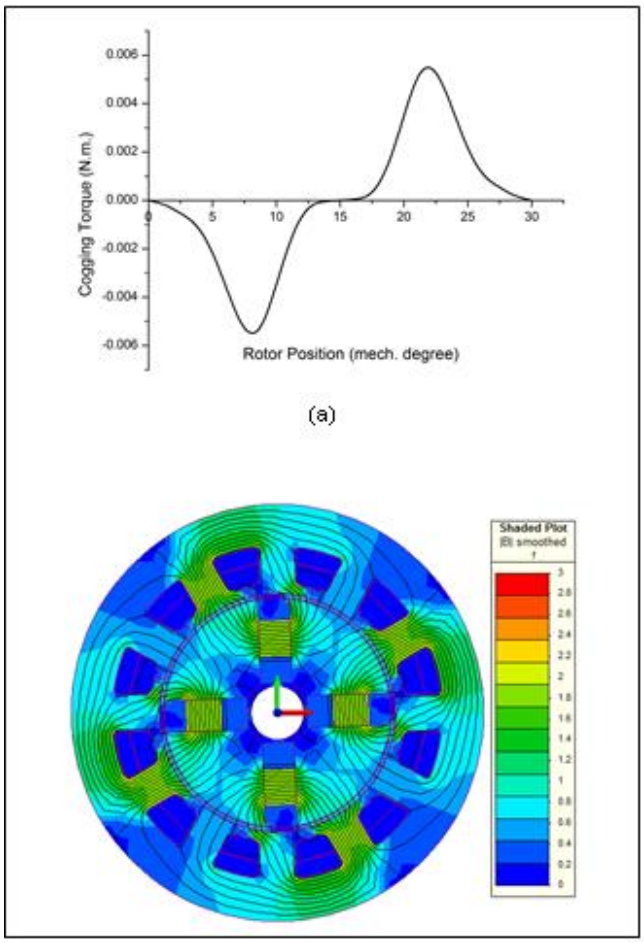

Fig. 4. *(a) Cogging torque profile, (b) Flux density plot of 2 kW reference motor.*

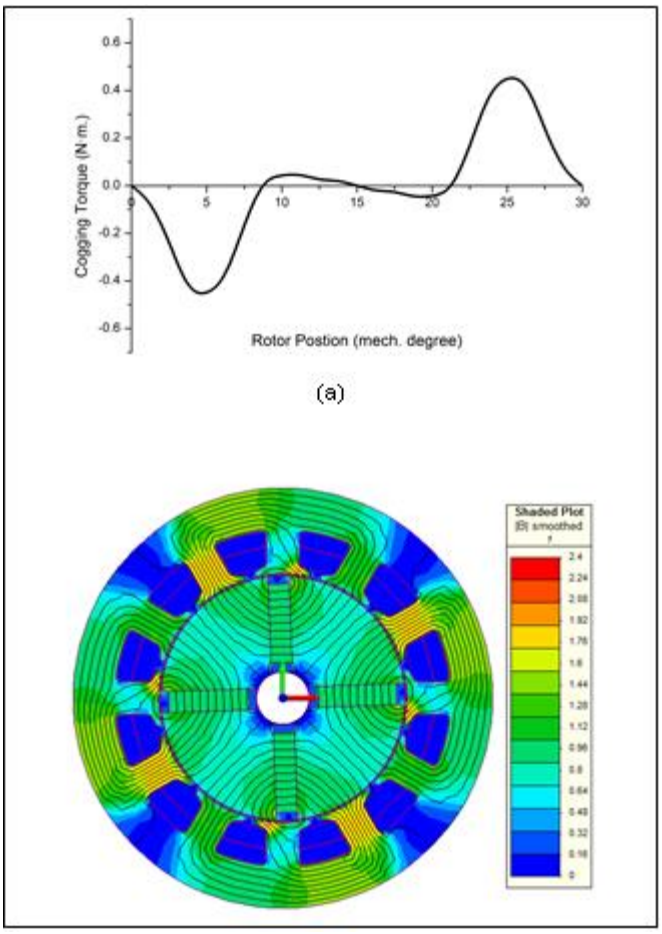

Fig. 5*. (a) Cogging torque profile, (b) Flux density plot of 5 kW reference motor.*

Cogging torque profiles are plotted according to recorded results. Cogging torque profile and flux density plot of reference 2 kW IPMSM obtained from FEA are depicted in Fig. 4(a) and Fig. 4(b) respectively. This reference 2 kW IPMSM has cogging torque of 0.01054 N.m. varying from peak to peak. It is observed that the flux density assumed in the motor's magnetic sections is close to actual flux density.

Cogging torque profile and flux density plot of reference 5 kW IPMSM is shown in Fig. 5(a) and Fig. 5(b) respectively. This reference 5 kW IPMSM has cogging torque of 0.897 N.m. varying from peak to peak. It is observed that the flux density assumed in the motor's magnetic sections is close to actual flux density.

Cogging torque profile and flux density plot of reference 120 kW IPMSM obtained from FEA are displayed in Fig. 6(a) and Fig. 6(b) respectively. This reference 120 kW IPMSM has cogging torque of 21.2724 N.m varying from peak to peak. It is observed that the flux density assumed in the motor's magnetic sections is close to actual flux density.

3. BASICS OF COGGING TORQUE

It is also known as no current or detent torque. It is inherently generated by changing of reluctance between the stator teeth and rotor's magnetic field. It is expressed by,

$$T_{cogg.} = -\frac{1}{2}\phi_g^2 \frac{dr}{d\theta} \quad (1)$$

Where flux in the air gap is ϕ_g , dr is reluctance in the air gap and $d\theta$ denotes rotor position. This equation provides support to the fundamentals that cogging torque is the association between stator teeth and rotor side permanent magnets. Cogging torque is periodically repeated because of the periodical variation in air-gap reluctance. Equation (2) expresses cogging torque in form of Fourier series [2].

$$T_{cogg.} = \sum_{i}^{\infty} T_{mi} \sin(mi\theta) \quad (2)$$

Where m denotes the LCM(least common multiple) of the number of poles and number of slots, i is an integer and T_{mi} is the Fourier coefficient. The cogging torque have a direct relation with total number of magnetic poles, stator slots and also have m numbers of periods per mechanical rotation of the rotor. From above equations it is clear that by lowering the values of ϕ_g (air-gap flux) or $dr/d\theta$ (rate of change of the air-gap reluctance)

reduction in cogging torque can be obtained. Since air-gap flux is required for torque generation. Therefore it is not appropriate to decrease the value of ϕ_g . Therefore, cogging torque can be reduced only by making air-gap reluctance constant with respect to rotor position [2].

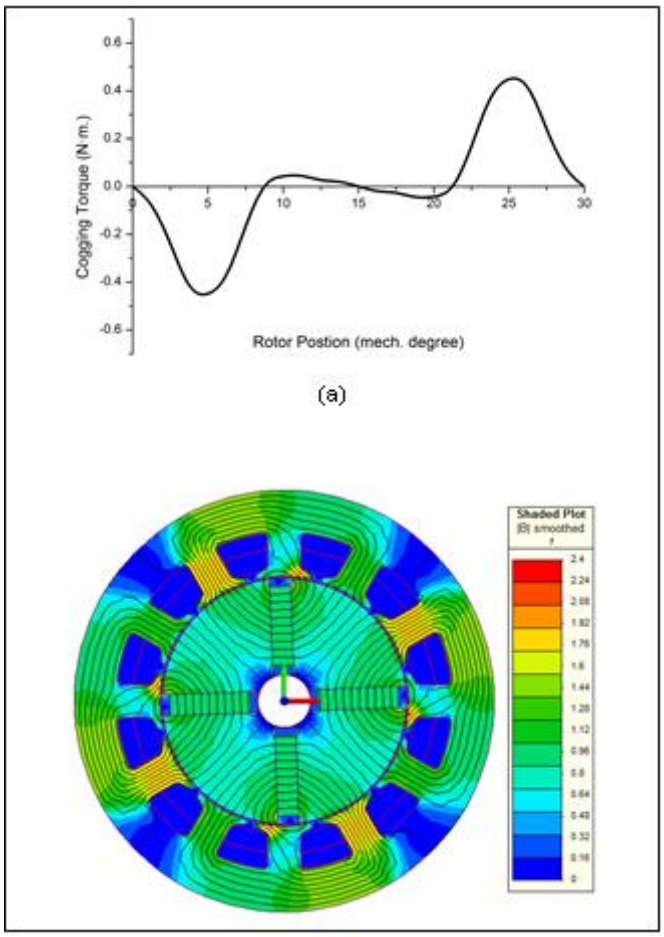

Fig. 6*. (a) Cogging torque profile, (b) Flux density plot of 120 kW reference motor.*

4. CORE EDGE INSET RADIUS VARIATION TECHNIQUE CONCLUSION

Core edge inset radius (CEIR) specifies the radius of the fillet located at the inside corners of the core bridge. Figure 7 shows cross-sectional view and enlarged quadrant view of rotor after applying CEIR variation technique. There are two different fillets on each side at inside corner of Core Bridge in every groove. The radius of each fillet can be increased till both the fillet will share same centre. The following subsections illustrate the effects of this modification on the different rating motors.

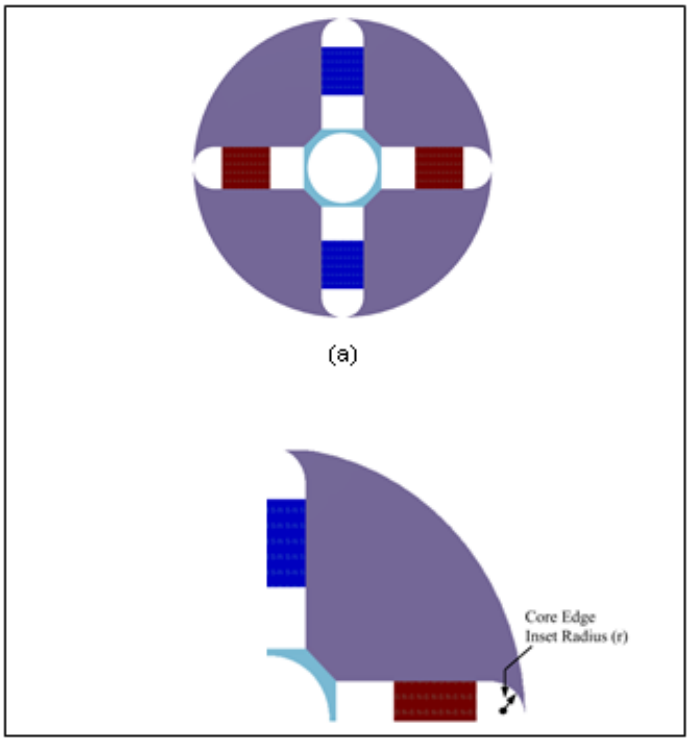

Fig. 7*. Showing core edge inset radius variation technique (a) cross-sectional view of rotor, (b) Enlarged quadrant structures of rotor.*

4.1 2 kW, 2,00,000 rpm IPMSM

Based on sizing equations 2 kW, 2,00,000 rpm a radial flux IPM motor is designed. For whole design a CAD algorithm is developed. Finite Element Analysis (FEA) is carried out on the motor model designed on the bases of information provided by the CAD algorithm.

Peak to peak cogging torque of initial 2 kW motor is 0.01054 N.m. Core edge inset radius variation is performed to improve design. Keeping other parameters unaffected only the value of core edge inset radius is changed from 0 to 1.5 mm. And to obtain the cogging torque profiles FEA is performed.

TABLE 2

EFFECT OF CEIR VARIATION ON COGGING TORQUE OF 2 KW, 2,00,000 RPM MOTOR

Core Edge Inset Radius (*mm*)	Torque (*N.m.*)	Cogging Torque (p-p) (*N.m.*)
Initial	0.095	0.01054
0.1	0.0933	0.009
0.5	0.0925	0.00793
1	0.0893	0.00657
1.5	0.0842	0.00534

Cogging torque reduced by the application and variation of CEIR is shown in Fig. 8(a). And Fig. 8(b) shows the torque profile comparison of initial and improved (with 1.5 mm CEIR) 2 kW IPMSM. From Table. 2 it is clear that minimum value of peak

to peak cogging torque is obtained at 1.5 mm CEIR. And as a result 49% reduction in the value of cogging torque is obtained (0.01054 N.m. to 0.00534 N.m.) with a marginal reduction of 11% in average torque.

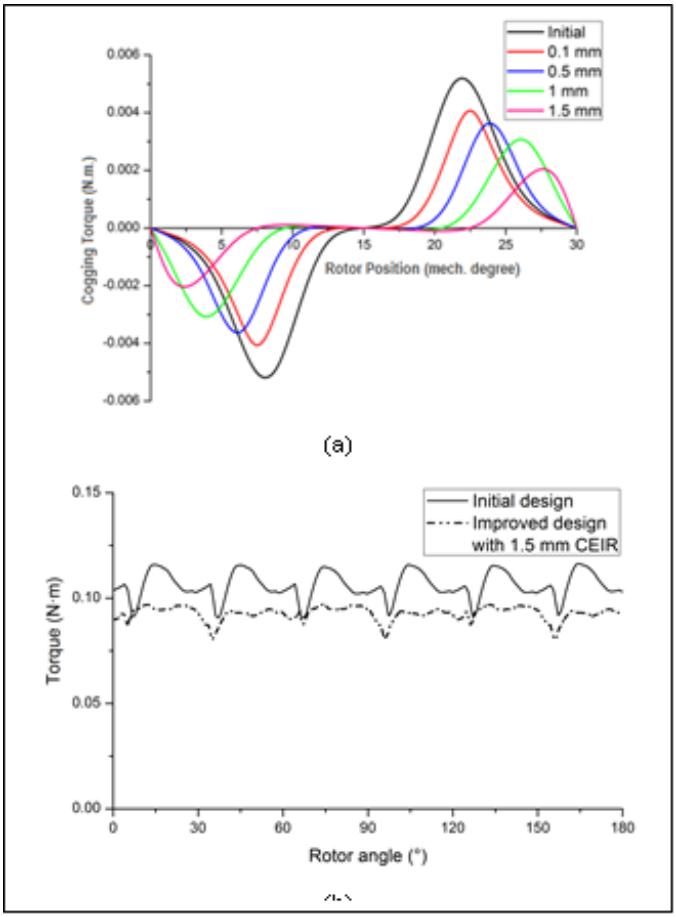

***Fig. 8**. Results of CEIR variation for 2 kW IPMSM. (a) Cogging torque profiles (b) Torque profile.*

The desirable result by CEIR variation technique is obtained at 1.5 mm. Back EMF profiles comparison of initial and improved 2 kW IPMSM is shown in Fig. 9(a). On account of core edge inset radius variation, quality of back emf is also improved. For 1.5 mm CEIR flux density in designed model is depicted in Fig. 9(b). Flux density observed in all the motor parts is as per assumption. Closeness between actual flux density and assumed flux density in various sections validate design.

4.2 5 kW, 24,000 rpm IPMSM

Based on sizing equations 5 kW, 24,000 rpm interior permanent magnet radial flux motor is designed. Finite Element Analysis (FEA) is carried out on the motor model designed on the bases of information provided by the CAD algorithm. Peak to peak cogging torque of initial 5 kW motor is 0.897 N.m. Core edge inset radius variation is performed keeping other parameters unaffected only the value of core edge inset radius is changed from 0 to 2 mm. And to obtain the cogging torque profiles FEA is performed. Cogging torque reduced by the application and variation of CEIR as shown in Fig 10(a). And Fig. 10(b) shows the torque profile comparison of initial and final models.

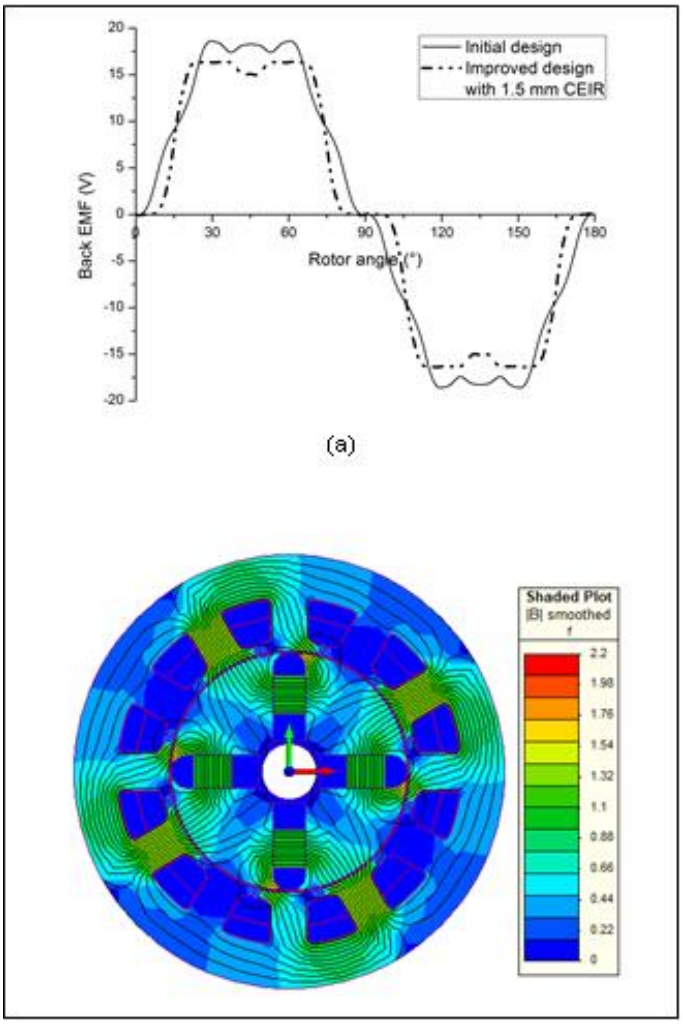

***Fig. 9**. Results of CEIR variation for motor 1. (a) Back EMF profiles, (b)Flux density plot of improved 2 kW IPMSM with 1.5 mm CEIR.*

TABLE 3

EFFECT OF CEIR VARIATION ON COGGING TORQUE OF 5 KW, 24,000 RPM MOTOR

Core Edge Inset Radius (*mm*)	Torque (*N.m.*)	Cogging Torque (p-p) (*N.m.*)
Initial	2	0.897
0.5	1.99	0.73
1	1.93	0.667
1.5	1.88	0.69
2	1.9	0.635

From Table. 3 it is clear that minimum value of peak to peak cogging torque is obtained at 2 mm CEIR. It is observed that 29% reduction in the value of cogging torque is obtained (0.897 N.m. to 0.635 N.m.) with a marginal reduction of 5% in average torque. The desirable result by CEIR variation technique is obtained at 2 mm. Back EMF profiles comparison of initial and improved 5 kW IPMSM is shown in Fig. 11(a).

On account of CEIR variation, quality of back emf is also improved. For 2 mm CEIR flux density in designed model is

depicted in Fig. 11(b). Flux density observed in all the motor parts is as per assumption. Closeness between actual flux density and assumed flux density in various sections validate design.

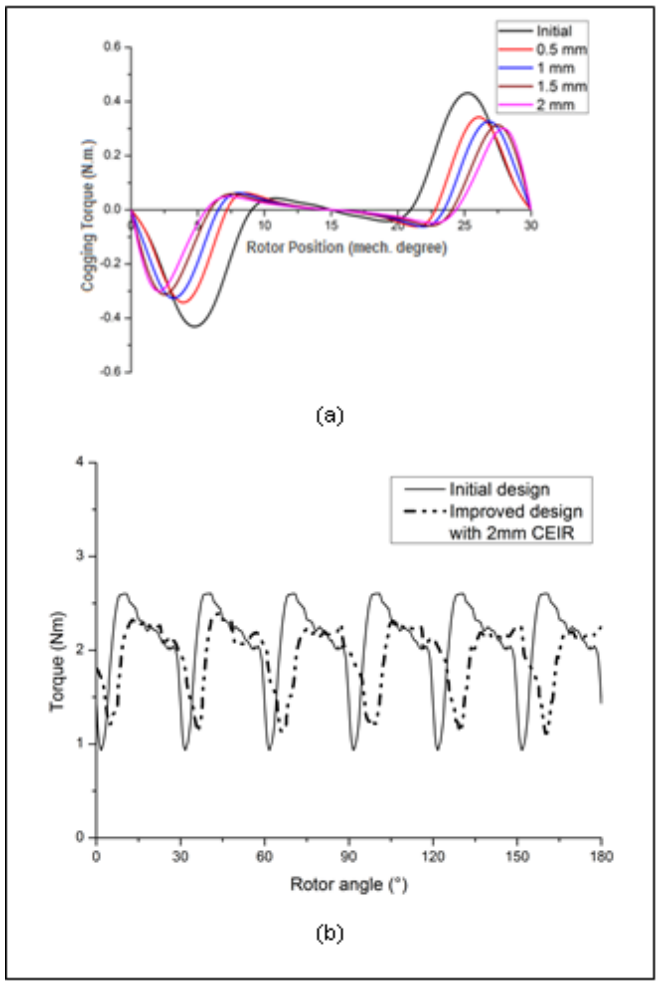

***Fig. 10**. (a) Shows Cogging torque and (b) Torque profile comparison of initial and improved (with 2 mm CEIR) 5 kW IPMSM.*

4.3 120 kW, 10,000 rpm IPMSM

Based on sizing equations 120 kW, 10,000 rpm radial flux interior permanent magnet motor is designed. For whole design a CAD algorithm is developed. Finite Element Analysis (FEA) is carried out on the motor model designed on the bases of information provided by the CAD algorithm.

Peak to peak cogging torque of initial 120 kW motor is 21.2724 N.m. Core edge inset radius variation is performed to improve design. Keeping other parameters unaffected only the value of core edge inset radius is changed from 0 to 0.456 mm. And to obtain the cogging torque profiles FEA is performed. Cogging torque reduced by the application and variation of CEIR as shown in Fig 12(a). And torque profile comparison of initial and improved 120 kW IPMSM is depicted in Fig. 12(b).

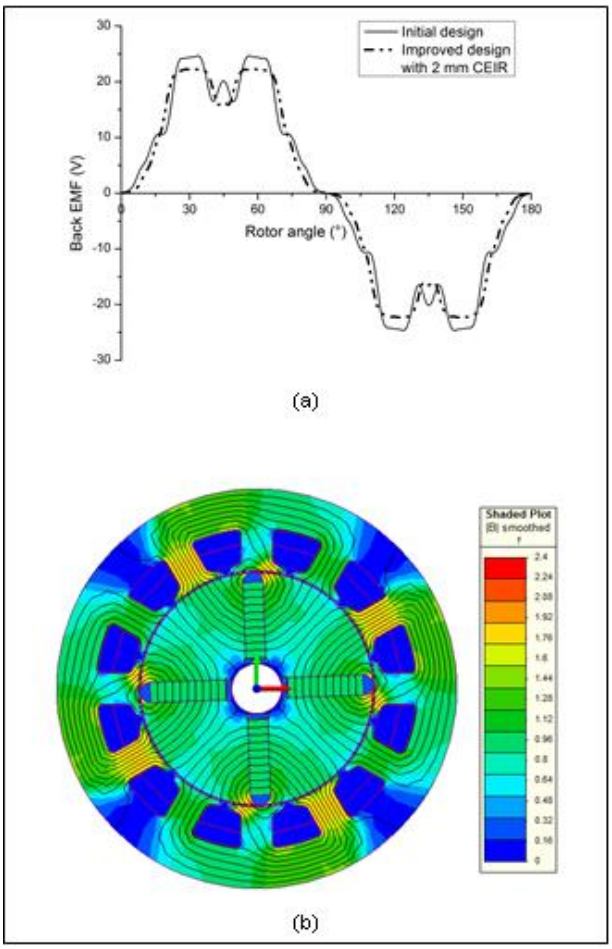

***Fig. 11**. Results of CEIR variation for motor 1. (a) Back EMF profiles, (b) Flux density plot of improved 5 kW IPMSM with 2mm CEIR.*

TABLE 4

EFFECT OF CEIR VARIATION ON COGGING TORQUE OF 120 KW, 10,000 RPM MOTOR

Core Edge Inset Radius (*mm*)	Torque (*N.m.*)	Cogging Torque (p-p) (*N.m.*)
Initial	115	21.2724
0.1	113	20.5393
0.2	112	19.3191
0.3	113	16.3
0.456	113	14.7145

From Table. 4 it is clear that minimum value of peak to peak variation in cogging torque is obtained at 0.456 mm CEIR. It is observed that 30% reduction in the value of cogging torque is obtained (21.2724 N.m. to 14.7124 N.m.) with a marginal reduction of 2% in average torque. The desirable result by CEIR variation technique is obtained at 0.456 mm. Back EMF profiles comparison of initial and improved 120 kW IPMSM is shown in Fig. 13(a). On account of CEIR variation, quality of back emf is improved. For 0.456 mm CEIR flux density in designed model is depicted in Fig. 13(b). Flux density observed in all the motor

parts is as per assumption. Closeness between actual flux density and assumed flux density in various sections validate design.

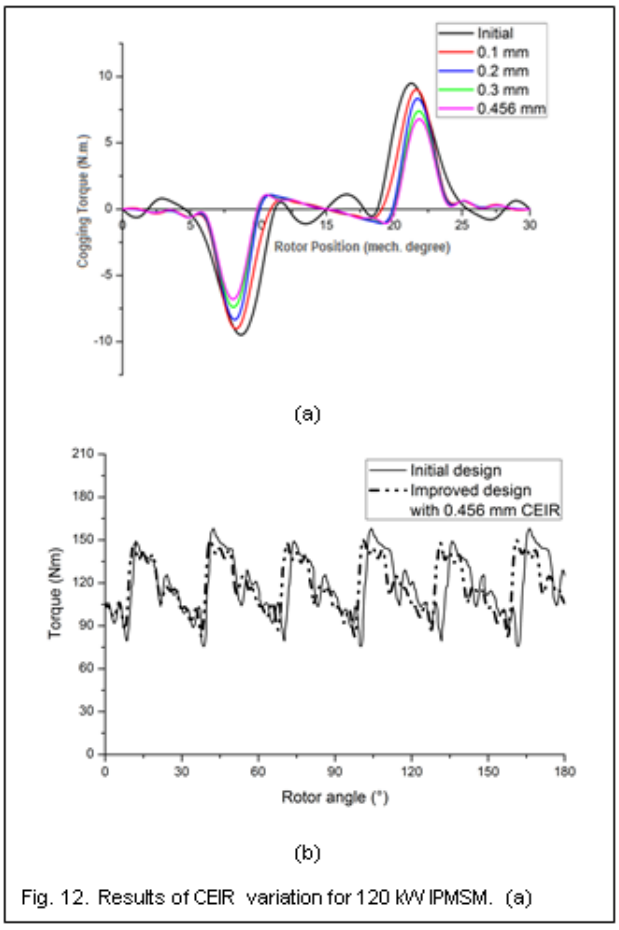

Fig. 12. Results of CEIR variation for 120 kW IPMSM. (a)

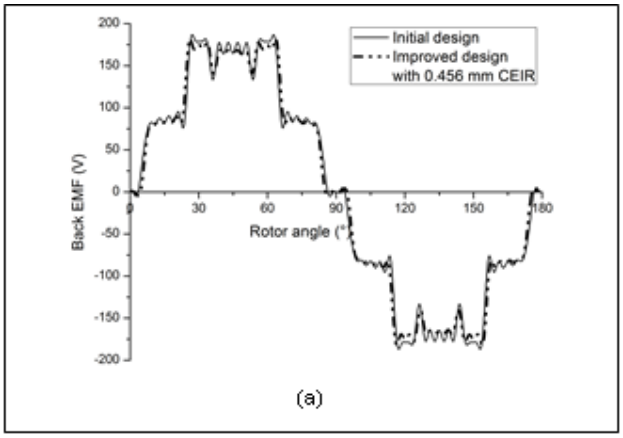

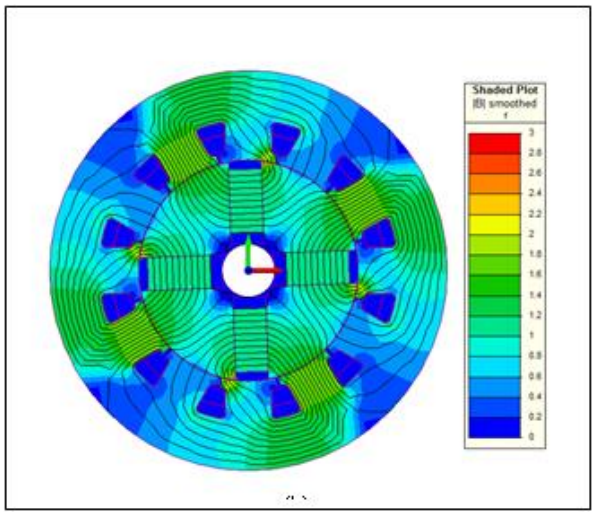

Fig. 13. *Results of CEIR variation for motor 1. (a) Back EMF profiles, (b)Flux density plot of improved 120 kW IPMSM with 0.456 mm CEIR.*

5 CONCLUSION

It is very important to reduce the cogging torque for the performance improvement of IPMSM. CEIR variation technique is applied to obtain the reduction in cogging torque for three different IPMSMs. These three different rating IPMSMs are considered in analysis to assess the effectiveness of CEIR variation technique on cogging torque reduction in wide range. CEIR value is changed while other design constraints are kept untouched for all ratings of IPMSM and finite element modeling, simulation & analysis are used to analyze its effect on cogging torque. Cogging torque is reduced by 49 % in 2 kW, 2,00,000 rpm motor, 29 % in 5 kW, 24,000 rpm motor, 30 % in 120 kW, 10,000 rpm motor. Cogging torque has been significantly reduced in all three cases with marginal variation in the value of average torque. The value of CEIR varies with motor's rating and its design parameters. According to design variations and subsequent analysis, proper value of core edge inset radius must be selected by the designer for better performance. The results confirm that CEIR variation technique is useful technique in cogging torque reduction of IPMSMs.

REFERENCES

[1] M. Sahebjam, M. B. Bannae Sharifian, M. R. Feyzi and M. Sabahi, "Novel Unified Control method of IM and PMSM," International Journal of Engineering (IJE), IJE Transactions B: Applications, vol. 32, No. 2, pp. 256-269, 2019. (IJE Transactions)

[2] M. Si, X.Yu Yong, S. Wei Zhao and S. Gong, "Design and analysis of a novel spoke-type permanent magnet synchronous motor," IET Electric Power Applications, vol. 10, no. 6, pp. 571-580, 2016. (IET Journals)

[3] A. N. Patel and A. Kapil, "Effect of magnet retaining sleeve thickness on cogging torque of radial flux permanent magnet brushless DC motor," 2016 International Conference on Emerging Trends in Engineering, Technology and Science, pp. 1-3, 2016. (Conference proceedings)

[4] D. C. Hanselman, Brushless Permanent Magnet Motor Design, New York, McGrow-Hill, 1994. (Book style)
[5] X. Jiang, J. Xing, Y. Li, and Y. Lu, "Theoretical and simulation analysis of influences of stator tooth width on cogging torque of BLDC motors," IEEE Transactions on Magnetics, vol. 45, no. 10, pp. 4601–4604, 2009. (IEEE Transactions)
[6] Z. Azar, Z.Q. Zhu, and G.Ombach, "Investigation of torque-speed characteristics and cogging torque of fractional-slot IPM brushless AC machines having alternate slot openings," IEEE Transactions on Industry Applications, vol. 48, no. 3, pp. 903–912, 2012. (IEEE Transactions)
[7] D. Wang, X. Wang, M. K. Kim, and S. Y. Jung, "Integrated optimization of two design techniques for cogging torque reduction combined with analytical method by a simple gradient descent method," IEEE Transactions on Magnetics, vol. 48, no. 8, pp. 2265-2276, 2012. (IEEE Transactions)
[8] N. Bianchi and S. Bolognani, "Design techniques for reducing the cogging torque in surface-mounted PM motors," IEEE Transactions on Industry Applications, vol. 38, no. 5, pp. 1259–1265, 2002. (IEEE Transactions)
[9] D. Wang, X. Wang, Y. Yang, and R. Zhang, "Optimization of magnetic pole shifting to reduce cogging torque in solid-rotor permanent-magnet synchronous motors," IEEE Transactions on Magnetics, vol. 46, no. 5, pp. 1228-1234, 2010. (IEEE Transactions)
[10] S. M. Hwang, J. B. Eom, Y. H. Jung, D.W. Lee, and B. S. Kang, "Various design techniques to reduce cogging torque by controlling energy variation in permanent magnet motors," IEEE Transactions on Magnetics, vol. 37, no. 4, pp. 2806–2809, 2001. (IEEE Transactions)
[11] D. C. Hanselman, "Effect of skew, pole count and slot count on brushless motor radial force, cogging torque and back EMF," IEEE Proceedings- Electric Power Applications, vol. 144, no. 5, pp. 325–330, 1997. (IEEE Proceedings)
[12] C. L. Xia, Z. Zhang, and Q. Geng, "Analytical modeling and analysis of surface mounted permanent magnet machines with skewed slots," IEEE Transactions on Magnetics, vol. 51, no. 5, pp. 1-8, 2015. (IEEE Transactions)
[13] Sang Moon Hwang, J. B. Eom, Y. H. Jung, D. W. Lee, and B. S. Kang, "Various design techniques to reduce cogging torque by controlling energy variation in permanent magnet motors," IEEE Transactions on Magnetics, vol. 37, no. 4, pp. 2806-2809, 2001. (IEEE Transactions)
[14] W. Fei, P. C. K. Luk, J. X. Shen, B. Xia, and Y. Wang, "Permanent magnet flux-switching integrated starter generator with different rotor configurations for cogging torque and torque ripple mitigations," IEEE Transactions on Industry Applications, vol. 47, no. 3, pp. 1247–1256, 2011. (IEEE Transactions)
[15] T. Li and G. Slemon, "Reduction of cogging torque in permanent magnet motors," IEEE Transactions on Magnetics, vol. 24, no. 6, pp. 2901–2903, 1988. (IEEE Transactions)
[16] T. Tudorache and I. Trifu, "Permanent-magnet synchronous machine cogging torque reduction using a hybrid model," IEEE Transactions on Magnetics, vol. 48, no. 10, pp. 2627–2632, 2012. (IEEE Transactions)
[17] G. Park, Y. Kim and S. Jung, "Design of IPMSM Applying V-Shape Skew Considering Axial Force Distribution and Performance Characteristics According to the Rotating Direction," IEEE Transactions on Applied Superconductivity, vol. 26, no. 4, pp. 1-5, 2016. (IEEE Transactions)
[18] X. Ge, Z. Q. Zhu, G. Kemp, D. Moule and C. Williams, "Optimal Step-Skew Methods for Cogging Torque Reduction Accounting for Three-Dimensional Effect of Interior Permanent Magnet Machines," IEEE Transactions on Energy Conversion, vol. 32, no. 1, pp. 222-232, 2017. (IEEE Transactions)